# Extending Two-Dimensional Human-Inspired Bipedal Robotic Walking to Three Dimensions through Geometric Reduction

Ryan W. Sinnet and Aaron D. Ames

***Abstract*— Three-dimensional humanlike bipedal walking is obtained through a hybrid control strategy which combines geometric reduction with human-inspired control. Functional Routhian reduction decouples the sagittal and coronal dynamics of a biped, thereby reducing the control design problem to sagittal motion. Experimental human kinematics data have shown that certain outputs on a human's kinematics follow a *canonical human function*: Human-inspired controllers are designed based on this function. The parameters of these functions are found through optimization by trying to make them as close to the human data as possible while simultaneously forming a partial hybrid zero dynamics under feedback linearization. PD control is used in these controllers to track the human functions resulting in stable walking in both two- and three-dimensional simulations.**

## I. INTRODUCTION

Bipedal robotic walking has been studied from a variety of perspectives. Existing approaches involve passivity-based control [1], [2], hybrid zero dynamics [3], [4], central pattern generators [5], [6], and compliance-based control [7]. Many of these schemes have proven effective and some have drawn inspiration from human walking in a holistic sense, yet the inituition behind these methods does not come directly from analysis of human walking data. Moreover, bipedal walking is difficult in two dimensions and extending it to three dimensions only further complicates the problem.

Biomechanics researchers are often interested in forces and dynamics [8]. Such analyses are useful in the design of prostheses yet fail to give a complete picture of human walking. While many studies have been conducted in the context of biomechanics [9], few have been done with respect to control engineering [10], [11]. This paper attempts to bridge the gap by proving insight from the viewpoints of both control and biomechanics.

When studying the biomechanics of walking, researchers use force plates and force loading models to measure and estimate the distribution of musculoskeletal forces and ground reaction forces [12]. These are used in conjunction with either inverse-dynamic models [13], [14] or forward-dynamic models [15], [16]. This paper instead analyzes functions representing outputs on the kinematics of a human. Recent methods [17], [18] draw from human data to achieve walking in robotic models. This paper extends [18] by introducing the notion of a hybrid zero dynamics for the sagittal control and then extending the sagittal gait to three dimensions.

R. W. Sinnet is an NSF Graduate Research Fellow. This work supported by NSF grant CNS-0953823 and NHARP award 00512-0184-2009.

Department of Mechanical Engineering, Texas A&M University, 3123 TAMU, College Station, TX 77843-3123 {rsinnet,aames}@tamu.edu

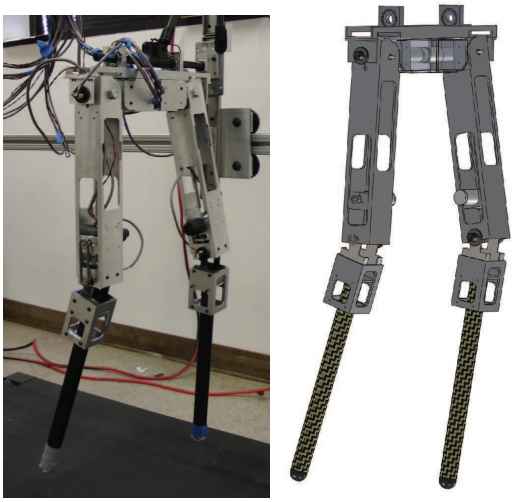

Fig. 1: The model of interest is based on the robot AMBER.

Starting with kinematics data from a human walking experiment, controllers are designed using a single class of mathematical functions termed *canonical human functions* which attempt to represent the fundamental behaviors of human walking. A state-based parameterization is introduced to remove time dependence and PD control is used to track these functions. This leads to an autonomous feedback control law which results in stable, humanlike walking in two dimensions.

After achieving two-dimensional walking, *functional Routhian reduction* is used to migrate this controller to a three-dimensional biped. To do this, two control laws are designed: The first shapes the Lagrangian of the three-dimensional biped so that it is amenable to reduction. The second uses feedback linearization to drive the system to the surface where reduction is valid. The end result will be stable walking for the three-dimensional model based on AMBER (shown in Fig. 1). Moreover, simulation results show that the two- and three-dimensional gaits are virtually identical.

The rest of this paper is structured as followed: Sec. II introduces the robotic model of interest. Sec. III presents the framework of human-inspired control, describing how to obtain feedback control laws—for a two-dimensional, sagittal plane robotic model—which result in stable walking in two dimensions. Sec. IV describes how to use the two-dimensional walking control laws developed in Sec. III to achieve three-dimensional walking. Sec. V provides simulation results for the three-dimensional model. The paper ends with Sec. VI which mentions related results and future research ideas.

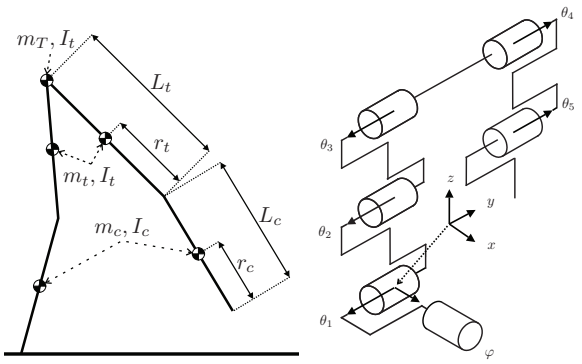


(a) Physical configuration. (b) Configuration variables.

Fig. 2: Bipedal robot of interest.

## II. ROBOTIC MODEL

The model of interest has point feet, knees, and a hip (comparable models have been considered [19], [20]) and is shown in Fig. 2(a)—this model represents an actual robot, AMBER, and, due to space constraints, the parameter values are omitted but are available online [21]. The robot will be modeled by the hybrid control system (see [22])

$$\mathscr{HC}_{3\mathrm{D}} = (\mathcal{D}_{3\mathrm{D}}, \mathcal{U}_{3\mathrm{D}}, \mathcal{S}_{3\mathrm{D}}, \Delta_{3\mathrm{D}}, f_{3\mathrm{D}}, g_{3\mathrm{D}}). \tag{1}$$

The body coordinates are chosen to be the relative angles between successive links. Combining the body coordinates with additional angular coordinates at the foot results in coordinates, $q = (\varphi, \theta^T)^T \in \mathcal{Q}_{3\mathrm{D}}$, as shown in Fig. 2(b); this intrinsically assumes the stance foot is pinned to the ground which simplifies the continuous dynamics.

**Hybrid Model Construction.** The hybrid model $\mathscr{HC}_{3\mathrm{D}}$ is easily constructed using the definitions of [19]. The unilateral constraint, $h_{3\mathrm{D}}(q)$, representing the height of the swing foot leads to domain $\mathcal{D}_{3\mathrm{D}}$ and guard $\mathcal{S}_{3\mathrm{D}}$. A Lagrangian $\mathcal{L}_{3\mathrm{D}} : T\mathcal{Q}_{3\mathrm{D}} \to \mathbb{R}$ can be derived from the physical configuration of the model and this can be written as the control system $(f_{3\mathrm{D}}, g_{3\mathrm{D}})$. From this Lagrangian, a dynamic model can be derived using standard techniques [23]. The admissible control is chosen to be $\mathcal{U}_{3\mathrm{D}} = \mathbb{R}^6$ and the torque distribution map, $B_{3\mathrm{D}} : \mathcal{Q}_{3\mathrm{D}} \to \mathbb{R}^{6\times 6}$, is simply the identity matrix: $B_{3\mathrm{D}}(q) = I_{6\times 6}$. Note that actuation is assumed at the stance foot. While this is not a realistic assumption for a point foot biped, it has been found that modeling footed robots with point foot models and the assumption of actuation shows promising results when simulations are compared to experimental results [24].

In the bipedal walking literature, it is common to use stance/swing leg notation [25]; it can be more intuitive to think of control design for the legs in this context—the differences in behavior provide a natural way of transforming the design problem. Thus, the legs are "swapped" at impact with a state relabeling procedure, $\mathcal{R} : \mathcal{Q}_{3\mathrm{D}} \to \mathcal{Q}_{3\mathrm{D}}$.

**Sagittal Restriction.** The goal of this paper is to obtain three-dimensional walking by decoupling the dynamics of $\mathscr{HC}_{3\mathrm{D}}$ such that sagittal control can be implemented independent of the coronal dynamics. To design sagittal control laws for use with reduction, it is necessary to consider a two-dimensional counterpart of the three-dimensional model. This reduced-order model is obtained by applying a *sagittal restriction* to the full-order model to obtain

$$\mathscr{HC}_{2\mathrm{D}} = (\mathcal{D}_{2\mathrm{D}}, \mathcal{U}_{2\mathrm{D}}, \mathcal{S}_{2\mathrm{D}}, \Delta_{2\mathrm{D}}, f_{2\mathrm{D}}, g_{2\mathrm{D}}). \tag{2}$$

This is as simple as setting $\varphi = 0$ and projecting away this coordinate from the various elements of the hybrid model, $\mathscr{HC}_{3\mathrm{D}}$. Applying the sagittal restriction gives Lagrangian

$$\mathcal{L}_{2\mathrm{D}}(\theta, \dot\theta) = \mathcal{L}_{3\mathrm{D}}(q, \dot q)|_{\varphi=0} = \frac{1}{2}\dot\theta^T M_{2\mathrm{D}}(\theta)\,\dot\theta - V_\theta(\theta),$$

which is used to determine the control system $(f_{2\mathrm{D}}, g_{2\mathrm{D}})$. The admissible control is $\mathcal{U}_{2\mathrm{D}} = \mathbb{R}^5$. The unilateral constraint $h_{2\mathrm{D}}(\theta) = h_{3\mathrm{D}}(\varphi{=}0, \theta)$ leads to the domain $\mathcal{D}_{2\mathrm{D}}$ and guard $\mathcal{S}_{2\mathrm{D}}$. The reset map $\Delta_{2\mathrm{D}}$ is obtained with Jacobian

$$E_{2\mathrm{D}}(p_x, p_y, \theta) = \mathrm{RowBasis}\left(E_{3\mathrm{D}}(p_x, p_y{=}0, p_z, \varphi{=}0, \theta)\right).$$

## III. HUMAN-INSPIRED CONTROL

The effective decoupling between sagittal and coronal dynamics afforded by functional Routhian Reduction is integral to the control scheme posed in this work: it allows for sagittal control to be considered *independent of motion in the coronal plane*. This section, therefore, provides the framework to design and implement human-inspired controllers which result in walking for the sagittaly-restricted model given in (2). This control design procedure begins with examination of human data, from which a *human-inspired* sagittal controller is developed.

**Walking Experiment and Human Outputs.** An experiment was conducted with human test subjects in which positional measurements of various points on the subjects were taken with high-speed motion capture. An in-depth description of this experiment is given in [26]; the data are available online [27]. The goal of human-inspired control is to use these kinematics data to motivate the construction of specific outputs of the robot to consider for the purposes of control. In essence, the human control system is viewed as a "black box" and outputs are sought on the human data, i.e., functions of the kinematics (or angles), which are capable of describing human walking. Anaylsis of candidate functions yielded five mutually-exclusive outputs which together appear to faithfully represent human walking—this claim will be substantiated through controller design. These outputs are:

- **O1**: *forward hip velocity*, i.e., the velocity of the $x$-position of the hip,
- **O2**: *swing leg slope*, i.e., the tangent of the angle between the $z$-axis and the projection of the line connecting the swing ankle and hip,
- **O3**: *stance knee relative angle*,
- **O4**: *swing knee relative angle*,
- **O5**: *vertical torso angle*, the angle of the torso measured with respect to the vertical axis of the world frame.

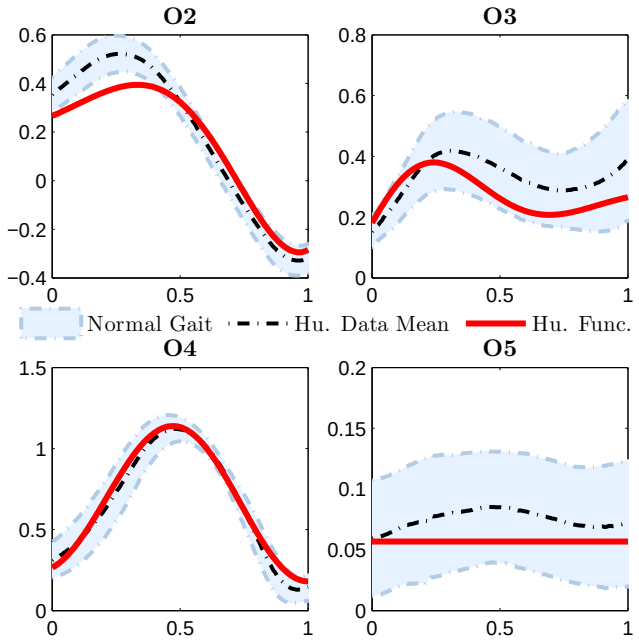


Fig. 3: Optimized human functions compared with normal human walking. Hip position is not shown as this varies depending on body size.

It is worth mentioning that the first output is a velocity rather than a position; this will be instrumental in achieving feedback control through parameterization of time.

In the biomechanics literature, it is typically assumed that walking is normally-distributed over a population of humans. Normal walking is typically defined as anything that falls within one standard deviation of the mean [28]. Using this definition of normal walking as a reference point, gaits designed can be examined to see if they are truly humanlike. Such a comparison is shown in Fig. 3 for the gait designed in this paper. The shaded areas represent normal human walking and were calculated by averaging the human data from the experiment described in this section (notice that the outputs in Fig. 3 are non-dimensional so averaging can be performed without normalization. One can see that the designed functions lie mostly within the shaded areas, thus confirming that the designed gait is relatively humanlike.

**Canonical Human Outputs.** In order to use the human outputs or functions just introduced, it is necessary to represent these outputs as continuous functions of time (rather than discrete, sampled data). This will allow the outputs of the robot, **O1**–**O5**, to be driven to these time-dependent human functions. It was discovered in [19], [29] that the considered human outputs can be accurately described by a *single* function—the time solution to a linear spring-mass-damper system—termed the *canonical human walking function*:

$$y_i^d(t,A) = e^{-a_{i,4}t}(a_{i,1}\cos a_{i,2}t + a_{i,3}\sin a_{i,2}t) + a_{i,5}, \quad (3)$$

where $i \in \{1,2,3,4,5\}$ is an index corresponding to outputs **O1**–**O5**. The parameters are combined into a matrix: $A = \{a_{i,j}\} \in \mathbb{R}^{5\times 5}$. Observe that (3) is the solution of a linear

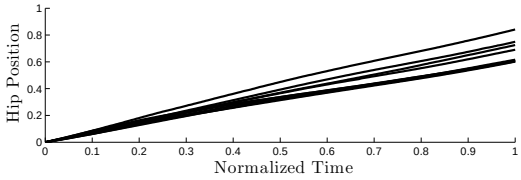


Fig. 4: Hip positions ($x$ coordinate) for nine different human test subjects.

spring-mass-damper system for which $a_{i,1}$ and $a_{i,3}$ would be determined from initial conditions, $a_{i,4} = \zeta\omega_n$ with damping ratio $\zeta$ and undamped natural frequency $\omega_n$, $a_{i,2} = \omega_d$ with damped natural frequency $\omega_d$, and $a_{i,5}$ is the gravity bias. It was shown in [29] that these functions can be fit to the human outputs with correlation coefficients near unity. It thus appears that humans act like linear spring-mass-damper systems with respect to the outputs chosen above. PD control will be used to track these functions, but first a parameterization will be introduced to replace time.

**Time-Invariant Parameterization.** The control strategy will attempt to track the human functions found through optimization. In order to achieve *autonomous* or *time-invariant* control, it is necessary to remove the time dependence from the human functions; this is accomplished by devising a state-based parameterization for time—a method that is common in the literature [3], [4].

Denote the parameterization by $\tau : \mathcal{Q}_{2D} \to \mathbb{R}_0^+$ where $\mathbb{R}_0^+$ represents time. For this parameterization to be accurate, it is necessary to find a function on the kinematics of the system which has an approximately linear relationship with time. Examination of the forward position of the hip, $p^x_{hip}$, in Fig. 4 reveals just such a relationship:

$$y_1^d(t,A) = a_{1,5} =: v^x_{hip}, \quad (4)$$

where $a_{1,1} = a_{1,2} = a_{1,3} = a_{1,4} = 0$ and $v^x_{hip} = \frac{\partial}{\partial\theta}p^x_{hip}(\theta)\,\dot\theta$ represents the hip velocity. Without loss of generality, assume time starts at 0 at the beginning of a step and let $\theta^- = \theta(t = 0)$ be the configuration of the robot at time $t = 0$. Then, the hip moves forward at an approximately constant rate so the relationship between velocity and position approximately satisfies $p^x_{hip}(t) \approx v^x_{hip}t + p^x_{hip}(\theta^-)$. This relationship motivates the following parameterization:

$$\tau(\theta) := \frac{p^x_{hip}(\theta) - p^x_{hip}(\theta^-)}{v^x_{hip}}. \quad (5)$$

**Sagittal Controller Construction.** The construction of the sagittal controller will consist of two steps: 1) find parameters of the canonical walking function (3) such that *hybrid zero dynamics* is achieved and 2) use these parameters together with PD control on the output functions to construct a controller that will result in walking in the two-dimensional robotic model.

**Hybrid Zero Dynamics.** The goal of the controller is to drive the outputs of the robot to the canonical human functions, thereby achieving humanlike trajectories. Therefore,

define the actual and desired outputs:

$$y_a(\theta) := \begin{bmatrix} p^x_{hip}(\theta) \\ m_{sw}(\theta) \\ \vartheta_{stk}(\theta) \\ \vartheta_{swk}(\theta) \\ \vartheta_{tor}(\theta) \end{bmatrix}, \; y_d(\tau(\theta)) := \begin{bmatrix} y^d_1(\tau(\theta), A) \\ y^d_2(\tau(\theta), A) \\ y^d_3(\tau(\theta), A) \\ y^d_4(\tau(\theta), A) \\ y^d_5(\tau(\theta), A) \end{bmatrix},$$

where $p^x_{hip}$, $m_{sw}$, $\vartheta_{sk}$, $\vartheta_{nsk}$ and $\vartheta_{tor}$ are the outputs **O1**–**O5** computed for the robot from its kinematics and $y^d_i$ are the canonical human walking functions (3) where time is parameterized by (5). For these outputs, the *zero dynamics surface* $\mathbf{Z}_A$ is parameterized by parameter matrix $A$, where the actual and desired outputs agree for all time, i.e., $y_a(\theta) \equiv y_d(\theta)$ for all time. Yet due to the nature of impacts, it is unlikely that the hip velocity will remain constant through impact; thus the *partial zero dynamics surface* $\mathbf{PZ}_A$ is also an important construct—this is the surface where $(y_a(\theta))_i \equiv (y_d(\theta))_i$, $i \in \{2, 3, 4, 5\}$ for all time. (See [29] for a more formal definition of these surfaces and why they are each individually important.)

The main result of [29] is that using the actual and desired outputs, $y_a$ and $y_d$, respectively, together with feedback linearization, it is possible to automatically determine a parameter matrix $A$ that results in stable walking. This is stated in the form of an optimization problem which uses the experimental human data as the cost function. From the mean human walking data, denote by $\tau^H[k]$ and $y^H_i[k]$ the sampled times and values, respectively, of the output functions **O1**–**O5**. Then define the cost function

$$\mathrm{Cost}_{\mathrm{HD}}(A) = \sum_{k=1}^{K} \sum_{i=1}^{5} \left( y^H_i[k] - y^d_i(t^H[k], A) \right)^2, \qquad (6)$$

which is simply the sum of residuals squared. Minimizing this cost results in the least squares fit of the canonical human walking functions to the mean human output data. In [29], a method was developed for expressing the zero dynamics surface, $\mathbf{Z}_A$, and partial zero dynamics surface, $\mathbf{PZ}_A$, *only* in terms of the parameter matrix $A$, thus motivating the optimization problem

$$A^* = \underset{A \in \mathbb{R}^{5\times 5}}{\operatorname{argmin}} \; \mathrm{Cost}_{\mathrm{HD}}(A) \qquad (7)$$

$$\text{s.t.} \quad \Delta_{2\mathrm{D}}(\mathcal{S}_{2\mathrm{D}} \cap \mathbf{Z}_A) \subset \mathbf{PZ}_A \qquad \text{(HZD)}$$

which depends only on the parameters $A$. Solving this optimization problem (numerically in MATLAB through `fmincon`) results in the matrix of parameters:

$$A^* = \begin{pmatrix} 0 & 0 & 0 & 0 & .6000 \\ .0241 & 9.5581 & .0806 & -3.8359 & .2422 \\ -.0767 & 13.341 & .1905 & 3.8029 & .2576 \\ -.4105 & -11.463 & -.1485 & -.2429 & .6759 \\ 0 & -19.651 & 0 & -17.750 & .0568 \end{pmatrix}$$

where $a_{1,5} = v^x_{hip}$ is chosen to be $0.6$ m/s, thus controlling the speed of the robot. The proximity of normal human walking to the human functions using parameter matrix $A^*$ is shown in Fig. 3. To reiterate an earlier point, these fits are quite close to normal human walking.

**PD Controller Design.** The main result of [29] is that the parameters, $A^*$, automatically result in bipedal robotic walking when feedback linearization is used. Yet the goal of this paper is different than [29]: in this paper, PD control is used as the reduction scheme posed in this paper requires that sagittal control be independent of lean ($\varphi$)—feedback linearization in general utilizes the entire state of the system. Motivated by these considerations, define the following control law

$$\mathcal{K}^A_{2\mathrm{D}}(\theta, \dot\theta) = k_p \begin{pmatrix} 0 \\ y_{d,2} - y_{a,2} \\ y_{d,3} - y_{a,3} \\ y_{d,4} - y_{a,4} \\ y_{d,5} - y_{a,5} \end{pmatrix} + k_d \begin{pmatrix} y_{d,1} - y_{a,1} \\ \dot y_{d,2} - \dot y_{a,2} \\ \dot y_{d,3} - \dot y_{a,3} \\ \dot y_{d,4} - \dot y_{a,4} \\ \dot y_{d,5} - \dot y_{a,5} \end{pmatrix}. \qquad (8)$$

In this paper, $k_p = 30$ and $k_d = 10$. This control law is applied to the system $\mathscr{HC}_{2\mathrm{D}}$ to obtain $\mathscr{H}^A_{2\mathrm{D}}$ which has vector field

$$f^A_{2\mathrm{D}}(\theta, \dot\theta) = f_{2\mathrm{D}}(\theta, \dot\theta) + g_{2\mathrm{D}}(\theta)\, \mathcal{K}^A_{2\mathrm{D}}(\theta, \dot\theta). \qquad (9)$$

**Simulation.** Simluation of $\mathscr{H}^A_{2\mathrm{D}}$ results in stable walking as expected. Fig. 5 shows the phase portrait which exhibits a closed trajectory—this limit cycle represents steady-state walking—as well as the torques and outputs. Of additional interest are the torques required to achieve the simulated results: these torques are reasonable for AMBER. The proximity of the system to the zero dynamics surface $\mathbf{Z}_A$ can also be seen. The humanlike nature of the gait can be seen in Fig. 6(a); specifically, the knee behavior is of paramount importance to human walking. Stability is confirmed by examining the eigenvalues of the Poincaré map linearized about the fixed point

$$\begin{aligned} \theta^*_{2\mathrm{D}} &= (-0.399, \; 0.330, \; 0.139, \; -0.316, \; 0.161), \\ \dot\theta^*_{2\mathrm{D}} &= (-1.613, \; 0.387, \; 1.463, \; 2.088, \; -4.615). \end{aligned}$$

The maximum eigenvalue is $\max_{i\in[1,|\Lambda|]} |\lambda_i| = .409$, which is below unity and therefore indicates a stable limit cycle.

## IV. FUNCTIONAL ROUTHIAN REDUCTION

Classical Routhian reduction [30] is a type of geometric reduction which leverages conserved momentum in the form of a constant to eliminate cyclic variables in a dynamical system. *Functional Routhian reduction* (first introduced in [31]) is a specific type of geometric reduction used in the presence of external forces (see [32]) in which the momentum map is set to a function rather than a constant. This reduction will decouple the sagittal and coronal dynamics; then, stable walking is obtained in three dimensions by applying control laws which give stable walking in the sagittally-restricted counterpart whose Lagrangian takes the structure of a functional Routhian [32, Eq. (13)].

Two controllers will be needed to obtain walking in the three-dimensional model in addition to the human-inspired controller. The first controller shapes the Lagrangian [32, Thm. 1] to into an almost-cyclic Lagrangian [32, Eq. (10)] which is amenable to reduction. In order to enjoy the decoupling effects of reduction, a second controller is needed to stabilize to the surface where reduction is valid.

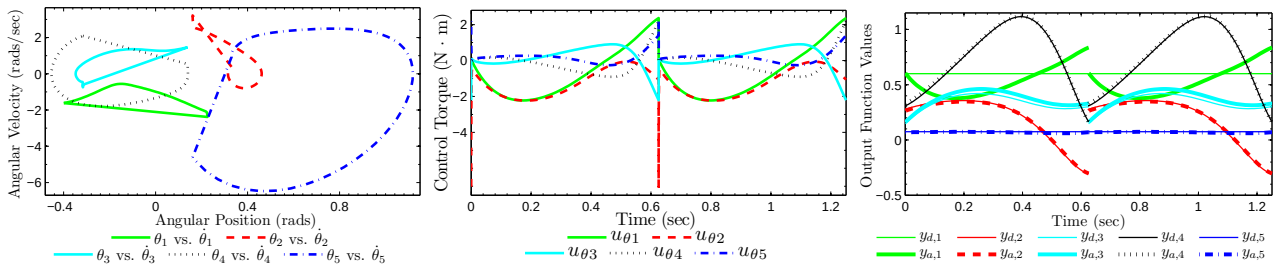


Fig. 5: Simulation of $\mathscr{H}^A_{2\mathrm{D}}$ from initial condition $(\theta^*_{2\mathrm{D}}, \dot{\theta}^*_{2\mathrm{D}})$: (l) phase portraits, (c) output torques, (r) output functions.

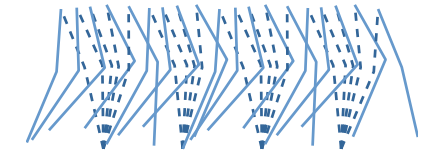

(a) 2D simulation.

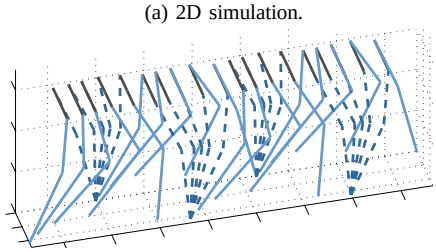

(b) 3D simulation.

Fig. 6: Simulated walking gaits. Hip in 6(b) shown in black, stance leg is dashed.

**Sagittal Control.** The first controller is strictly responsible for motion in the sagittal plane. This controller will be used with the reduction controllers to generate walking for the three-dimensional model. In Sec. III, a controller was described which resulted in walking for the sagittally restricted model $\mathscr{HC}_{2\mathrm{D}}$ given in (2). This exact control law, $\mathcal{K}^A_{2\mathrm{D}}$, given by (8), will be used for the three-dimensional model $\mathscr{HC}_{3\mathrm{D}}$ given in (1): $\mathcal{K}^A_{3\mathrm{D}}(q,\dot{q})) = \iota\left(\mathcal{K}^A_{2\mathrm{D}}(\theta,\dot{\theta})\right)$. Here, $\iota : \mathcal{U}_\theta \to \mathcal{U}_{3\mathrm{D}}$ is an embedding given by $u_\theta \mapsto (0, u_\theta)$.

**Lagrangian Shaping Controller.** A controller is needed to shape the Lagrangian $\mathcal{L}_{3\mathrm{D}}$ into an almost-cyclic Lagrangian, say $\mathcal{L}_\alpha$, where reduction is valid. In this paper, $\lambda(\varphi) = -\alpha\varphi$ is chosen with control gain $\alpha = 1$. The appropriate control law is given by [33, Eq. (4)] with control gain $\epsilon = 20$, and, when applied, results in the vector field

$$f^{A,\alpha}_{3\mathrm{D}}(q,\dot{q}) = f_{3\mathrm{D}}(q,\dot{q}) + g_{3\mathrm{D}}(q)\,\mathcal{K}^{A,\alpha}_{3\mathrm{D}}(q,\dot{q}).$$

For the proper initial conditions as specified in [33, Eq. (6)], the continuous dynamics of $\mathscr{HC}_{3\mathrm{D}}$ can be effectively decoupled into the sagittal and coronal dynamics with the control law $\mathcal{K}^{A,\alpha}_{3\mathrm{D}}(q,\dot{q})$ (cf. [33]). This control law contains the sagittal control law $\mathcal{K}_{2\mathrm{D}}(\theta,\dot{\theta})$. Furthermore, the dynamics of $\varphi$ evolve according to [33, Eq. (7)]. To guarantee the that initial condition assumption [33, Eq. (6)] is satisfied, an additional control law is needed. Feedback linearization is used to stabilize to the surface containing valid initial conditions. This motivates the output function

$$y_z(q,\dot{q}) := \dot{\varphi} + m_\varphi^{-1}(\theta)\left(\alpha\varphi + M_{\varphi,\theta}(\theta)\,\dot{\theta}\right),$$

which has relative degree 1. Driving this output to zero will cause the system to operate on an embedded submanifold known as the zero dynamics manifold:

$$\mathcal{Z} := \left\{\begin{pmatrix} q^T, \dot{q}^T \end{pmatrix} \in T\mathcal{Q}_{3\mathrm{D}} : y_z(q,\dot{q}) = 0\right\}.$$

The control law that is sought is well-defined under the framework of feedback linearization [34]. Applying this control law yields the vector field $f^{A,\alpha,\epsilon}_{3\mathrm{D}}(q,\dot{q})$. Using this vector field, one can construct a hybrid system implementing the described controllers: $\mathscr{H}^{A,\alpha,\epsilon}_{3\mathrm{D}} = (\mathcal{D}_{3\mathrm{D}}, \mathcal{S}_{3\mathrm{D}}, \Delta_{3\mathrm{D}}, f^{A,\alpha,\epsilon}_{3\mathrm{D}})$.

## V. Simulation Results

**Reduction Surface Stabilization.** Simluation of $\mathscr{H}^{A,\alpha,\epsilon}_{3\mathrm{D}}$ results in stable walking which is strikingly similar to simulation of $\mathscr{H}^A_{2\mathrm{D}}$ as can be seen from Fig. 7 which shows the phase portrait, the torques, and the outputs. Gait tiles are shown in Fig. 6(b). A linearization of the Poincaré map about the fixed point

$$\begin{aligned} q^* &= (-.00376,\ -.404,\ .329,\ .146,\ -.308,\ .145), \\ \dot{q}^* &= (-.126,\ -1.628,\ .399,\ 1.475,\ 2.112\ -4.351). \end{aligned}$$

yields maximum eigenvalue $\max_{i\in|\Lambda|}|\lambda_i| = 0.286$.

As before, the largest eigenvalue has magnitude below unity indicating stability. However, the magnitudes of eigenvalues only indicate that the manifold is locally attractive; thus the system may start close to a stable limit cycle, but not close enough to be within the region of attraction.

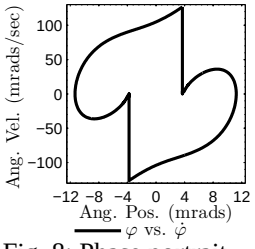


Fig. 8: Phase portrait, $\varphi$.

The most important observation is that the two-dimensional and three-dimensional walking gaits are virtually identical. Moreover, since the two-dimensional control law was used to construct the three-dimensional system, it appears that the sagittal and coronal dynamics are indeed decoupled which illustrates the value of function Routhian reduction.

## VI. Concluding Remarks

This paper presented a framework for achieving three-dimensional bipedal walking by using sagittal control design on a two-dimensional model. This framework, when applied to robotic models, allows one to obtain humanlike walking gaits with provable stability properties. Moreover, these gaits have the added benefit of being humanlike as measured by the closeness of the robot kinematics to human kinematics as described in Sec. III. Human-inspired control has been

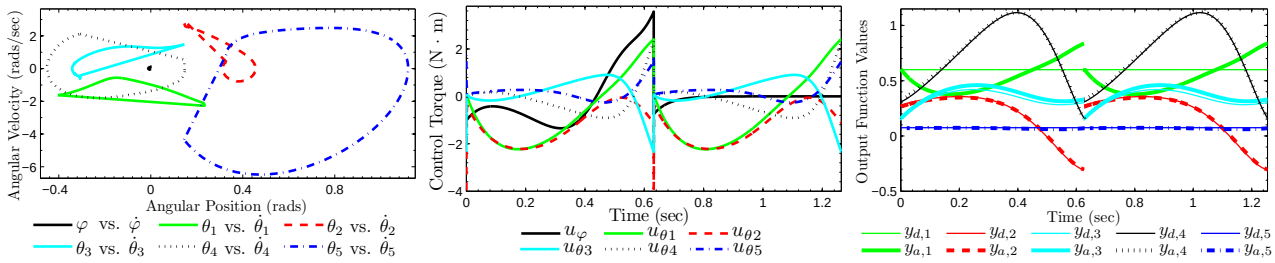


Fig. 7: Simulation of $\mathscr{H}_{3D}^{A,\alpha,\epsilon}$ from initial condition $(q_{3D}^*, \dot{q}_{3D}^*)$: (l) phase portraits, (c) output torques, (r) output functions.

the topic of recent research in which results have been validated experimentally. The novelty in this paper lies in the application of geometric reduction and sagittal PD control.

Finally, feedback linearization is generally not robust to model uncertainty. However, this control design has recently been validated on NAO despite the lack of feet in the hybrid model [24] and experiments on AMBER seem to confirm that human-inspired control provides sufficient robustness [35]. This allays these concerns to the extent that the walking is not unmanageably robust. Thus, it has become apparent that the union of functional Routhian reduction and human-inspired control results in promising, three-dimensional humanlike walking as well as a reduction in the complexity of the control design procedure as a ramification of the decoupling of the sagittal and coronal dynamics.

## REFERENCES


[1] M. W. Spong and F. Bullo, "Controlled symmetries and passive walking," *IEEE TAC*, vol. 50, no. 7, pp. 1025–31, 2005.

[2] S. Collins, A. Ruina, R. Tedrake, and M. Wisse, "Efficient bipedal robots based on passive-dynamic walkers," *Science*, vol. 307, pp. 1082–5, Feb. 2005.

[3] E. R. Westervelt, J. W. Grizzle, and D. E. Koditschek, "Hybrid zero dynamics of planar biped walkers," *IEEE TAC*, vol. 48, no. 1, pp. 42–56, Jan. 2003.

[4] E. R. Westervelt, J. W. Grizzle, C. Chevallereau, J. H. Choi, and B. Morris, *Feedback Control of Dynamic Bipedal Robot Locomotion*. Boca Raton: CRC Press, June 2007.

[5] T. Reil and P. Husbands, "Evolution of central pattern generators for bipedal walking in a real-time physics environment," *IEEE Trans. on Evolutionary Computation*, vol. 6, no. 2, pp. 159–68, Apr. 2002.

[6] K. Tsuchiya, S. Aoi, and K. Tsujita, "Locomotion control of a biped locomotion robot using nonlinear oscillators," in *IEEE/RSJ Intl. Conf. on Intelligent Robots and Systems*, Oct. 2003, pp. 1745–50.

[7] J. Pratt, P. Dilworth, and G. Pratt, "Virtual model control of a bipedal walking robot," in *IEEE Intl. Conf. on Robotics and Automation*, Albuquerque, Apr. 1997, pp. 193–8.

[8] D. A. Winter, *Biomechanics and Motor Control of Human Movement*, 2nd ed. New York: Wiley-Interscience, May 1990.

[9] D. H. Sutherland, K. R. Kaufman, and J. R. Moitoza, *Human Walking*, 3rd ed. Baltimore: Lippincott Williams & Wilkins, Dec. 2005, ch. Kinematics of Normal Human Walking, pp. 23–44.

[10] A. G. Bharatkumar, K. E. Daigle, M. G. Pandy, Q. Cai, and J. K. Aggarwal, "Lower limb kinematics of human walking with the medial axis transformation," in *IEEE Workshop on Motion of Non-Rigid and Articulated Objects*, Austin, Nov. 1994, pp. 70–6.

[11] V. M. Zatsiorsky, *Kinematics of Human Motion*, 1st ed. Champaign: Human Kinetics, Sept. 1997.

[12] S. H. Scott and D. A. Winter, "Biomechanical model of the human foot: Kinematics and kinetics during the stance phase of walking," *J. of Biomech.*, vol. 26, no. 9, pp. 1091–104, Sept. 1993.

[13] U. Glitsch and W. Baumann, "The three-dimensional determination of internal loads in the lower extremity," *J. of Biomech. Eng.*, vol. 30, no. 11, pp. 1123–31, Nov. 1997.

[14] S. Siegler and W. Liu, *Three-Dimensional Analysis of Human Locomotion*, 1st ed. New York: John Wiley & Sons, 1997, ch. Inverse Dynamics in Human Locomotion, pp. 191–209.

[15] F. C. Anderson and M. G. Pandy, "Dynamic optimization of human walking," *J. of Biomech. Eng.*, vol. 123, no. 5, pp. 381–90, Oct. 2001.

[16] R. R. Neptune, S. A. Kautz, and F. E. Zajac, "Contributions of the individual ankle plantar flexors to support, forward progression and swing initiation during walking," *J. of Biomech.*, vol. 34, no. 11, pp. 1387–98, Nov. 2001.

[17] S. Srinivasan, I. A. Raptis, and E. R. Westervelt, "Low-dimensional sagittal plane model of normal human walking," *J. of Biomech. Eng.*, vol. 130, no. 5, Oct. 2008.

[18] R. W. Sinnet, M. J. Powell, R. P. Shah, and A. D. Ames, "A human-inspired hybrid control approach to bipedal robotic walking," in *18th IFAC World Congress*, Milan, Sept. 2011, pp. 6904–11.

[19] R. W. Sinnet, M. J. Powell, S. Jiang, and A. D. Ames, "Compass gait revisited: A human data perspective with extensions to three dimensions," in *50th IEEE Conf. on Decision and Control and European Control Conf.*, Orlando, Dec. 2011, pp. 682–9.

[20] C. Chevallereau, J. W. Grizzle, and C. Shih, "Asymptotically stable walking of a five-link underactuated 3d bipedal robot," *IEEE TRO*, vol. 25, no. 1, pp. 37–50, Feb. 2009.

[21] R. W. Sinnet. (2012) Supplementary material for acc_2012_sa_01. [Online]. Available: http://rwsinnet.com/papers/acc_2012_sa_01/

[22] J. W. Grizzle, C. Chevallereau, A. D. Ames, and R. W. Sinnet, "3D bipedal robotic walking: models, feedback control, and open problems," in *IFAC Symposium on Nonlinear Control Systems*, Bologna, Sept. 2010.

[23] R. M. Murray, Z. Li, and S. S. Sastry, *A Mathematical Introduction to Robotic Manipulation*. Boca Raton: CRC Press, Mar. 1994.

[24] A. D. Ames, E. A. Cousineau, and M. J. Powell, "Dynamically stable bipedal robotic walking with NAO via human-inspired hybrid zero dynamics," in *Hybrid Systems: Computation and Control*, Beijing, Apr. 2012.

[25] J. W. Grizzle, G. Abba, and F. Plestan, "Asymptotically stable walking for biped robots: Analysis via systems with impulse effects," *IEEE TAC*, vol. 46, no. 1, pp. 51–64, Jan. 2001.

[26] A. D. Ames, R. Vasudevan, and R. Bajcsy, "Human-data based cost of bipedal robotic walking," in *14th Intl. Conf. on Hybrid Systems: Computation and Control*, Chicago, Apr. 2011, pp. 153–62.

[27] R. Vasudevan. (2011) Motion capture data for hybrid bipedal walking. [Online]. Available: http://eecs.berkeley.edu/~ramv/bipedaldata.html

[28] J. Perry and J. Burnfield, *Gait Analysis: Normal and Pathological Function*, 2nd ed. Thorofare: Slack Incorporated, 2010.

[29] A. D. Ames, "First steps toward automatically generating bipedal robotic walking from human data," in *In 8th Intl. Workshop on Robotic Motion and Control, RoMoCo'11*, Gronów, June 2011.

[30] J. E. Marsden and T. S. Ratiu, *Introduction to Mechanics and Symmetry*, ser. Texts in Applied Mathematics. Springer, 1999, vol. 17.

[31] A. D. Ames, "A categorical theory of hybrid systems," Ph.D. dissertation, University of California, Berkeley, 2006.

[32] R. W. Sinnet and A. D. Ames, "3D bipedal walking with knees and feet: A hybrid geometric approach," in *48th IEEE Conf. on Decision and Control*, Shanghai, Dec. 2009, pp. 3208–13.

[33] A. D. Ames, R. W. Sinnet, and E. D. B. Wendel, "Three-dimensional kneed bipedal walking: A hybrid geometric approach," in *12th ACM Intl. Conf. on Hybrid Systems: Computation and Control, Lecture Notes in Computer Science—HSCC 2009*, vol. 5469. San Francisco: Springer Verlag, Apr. 2009, pp. 16–30.

[34] S. S. Sastry, *Nonlinear Systems: Analysis, Stability and Control*. New York: Springer, June 1999.

[35] A. D. Ames. (2012) Robustness tests on the bipedal robot amber. [Online]. Available: http://youtu.be/RgQ8atV1NW0